Original Article

The effects of common house fly (*Musca domestica*) larvae-derived substances on wound healing in mouse model

Doaa E Said[1], Hoda M Khalifa[2], Lamia M El-Samad[3], Marwa A Meheissen[4], Hala E Diab[1], Radwa G Diab[1]

Departments of Medical Parasitology[1], Histology and Cell Biology[2], Zoology[3], Medical Microbiology and Immunology[4], Alexandria Faculties of Medicine[1,2,4] and Sceince[3], Egypt

ABSTRACT

Background: Maggot debridement therapy is a therapeutic wound myiasis that depends mainly on *L. sericata* larva. Owing to its availability and cheap breeding, *M. domestica* was suggested as an alternative to *Lucilia*.
Objective: The present study was designed to assess the role of *M. domestica* larvae-derived substances on wound healing in immunocompetent and immunosuppressed mice.
Material and Methods: Chitosan and gut extracts, obtained from *M. domestica* larvae, were applied daily on skin wounds of Swiss albino mice. Mice were divided into two groups, control non-treated mice (I), and experimental treated mice (II). Each group included immunocompetent (a), and immunosuppressed (b) mice. The experimental subgroups were treated with either chitosan (1) or gut extracts (2). Wounds were assessed by macroscopic evaluation, wound contracture, histopathological, immunohistochemical and bacteriological parameters.
Results: In control non treated mice hair growth was evident with normal underlying skin by the end of the experiment (4 weeks) except in immunosuppressed (Ib) subgroup. Significant reduction in wound size was detected on the 7th day post wounding (PW) in the immunocompetent-chitosan-treated subgroup (IIa1) compared to Ia, IIb1, and IIa2 subgroups. Histopathological examination showed early epidermal creeping on the 3rd day PW in IIa1, IIa2, and IIb2 subgroups. Significant increase in collagen deposition was best detected in both gut extract-treated subgroups (IIa2 and IIb2) compared to the control subgroups (Ia, and Ib). Strong immunohistochemical reaction was evident in all immunocompetent treated mice (IIa1 and IIa2) by the 7th day PW and in IIb2 by the 14th day PW. Delay in keratin maturation was detected in both control subgroups and IIb1. Significant reduction in staphylococcal colonies was detected by the 7th day PW in all immunosuppressed treated subgroups compared to their control subgroup (Ib).
Conclusion: The difference in the rapid wound closure as detected by chitosan treatment, and the effective skin architecting by gut extract treatment recommends further trial by their combined therapy.

Keywords: chitosan; debridement therapy; gut extract; housefly; immunocytokeratin; maggot.

Received: 17 October, 2022; **Accepted:** 23 December, 2022.

Corresponding Author: Radwa G. Diab, **Tel.:** +20 1005286226, **Email:** Radwa_gdiab@yahoo.com.

Print ISSN: 1687-7942, **Online ISSN:** 2090-2646, **Vol. 15, No. 3, December, 2022.**

INTRODUCTION

Maggot debridement therapy (MDT) is an ancient method for wounds treatment depending on the capability of maggots of certain higher Diptera for necrotic tissue debridement, wound disinfection and enhancement of granulation tissue formation[1]. The sense of repugnance, pain and wound malodour, in addition to the discovery of antibiotics, all led to limitations of the use of MDT by both patients and surgeons[2,3]. Thus, the replacement of live maggots with larval extracts responsible for the aforementioned functions in wound healing was indispensable.

Chitin and its N-deacetylation derivative, chitosan, are biopolymers that share in several industrial activities including the biomedical field. In the latter, they show promising roles in healing of chronic wounds, enhancement of immunity, in addition to their haemostatic, hypolipidaemic and antibacterial effects[4]. Insects, especially their cuticles and larvae, act as natural sources for chitin and chitosan with high biodiversity, and are obtained by simple, easy and cheap chitin extraction methods[5]. Chitosan was chosen among different maggot extracts since it has a considerable role in wound healing as previously reported in several studies over the last decade[4,6,7]. Different chitosan-based dressings and preparations are available such as nano-fiber membranes, powders, gels, sponges or as a composite[7]. Furthermore, larvae gut extract may promote wound healing due to its antibacterial and proteolytic properties[8].

It was observed that wound healing hierarchy works together with the immune system; and

 DOI:10.21608/PUJ.2022.169218.1190

that the achievement of proper healing could constitute a life-saving hope in individuals suffering immunosuppressive states as intensive cancer chemotherapy, blood disorders and organ transplantation. Moreover, malignancy and anti-cancer therapy are associated with immune problems that predispose patients to opportunistic infections. Deficient immune systems likely cause a decrease in cellular proliferation, neovascularization, and in matrix production[9].

The house fly *M. domestica* is an important sanitary pest insect recognized as a source of proteins, peptides, chitin and chitosan, phospholipids, and antibiotics, extracted from their larvae. Notably, chitin and chitosan were found mainly in larvae cuticles[5]. It is proposed due to its short life cycle (as short as 7-10 days in optimum temperature), high fecundity (up to 150 eggs/batch and up to 20 generations annually), and the simplicity and low cost of its rearing on a commercial base. Besides, *M. domestica* larvae also have an important role in digestion of organic wastes[10]. For the fore-mentioned discoveries in the field of *M. domestica* applications, and for being available in our everyday life, easy to collect and cheap to breed, we were challenged to assess the effectiveness of *M. domestica* larval-derived extracts of chitosan and gut contents on experimental wound healing. This prompted us to test the extracted compounds as potential alternatives to those derived from the widely used larvae of *L. sericata*. The present study was designed to assess the role of *M. domestica* larvae-derived chitosan and gut extracts on wound healing in immunocompetent and immunosuppressed experimental mice.

MATERIAL AND METHODS

This case-control study was conducted in Departments of Medical Parasitology, Microbiology, and Zoology, Faculties of Medicine, and Science, Alexandria University, Alexandria, Egypt during the period from July 2017-July 2018.

Study design: Chitosan and larvae gut extracts were prepared from *M. domestica* maintained cultures. Both substances were applied daily for 4 weeks on a wound in the skin on the back of immunocompetent and immunosuppressed Swiss Albino mice. In comparison to non-treated mice, observation of skin for signs of inflammation and wound healing was recorded, followed by measuring wound diameter for recording the degree of wound contracture. Other parameters included histopathological, immunohistochemical, and bacteriological studies.

Rearing *M. domestica*: Cultures of *M. domestica* adults were maintained at the laboratory of Zoology Department, Faculty of Science, University of Alexandria. Adults were identified depending on the shape of the posterior spiracles of the third instar larvae developed during rearing. Fresh beef liver was utilized for oviposition, and the liver containing eggs was used for cycle maintenance. The emerging larvae were used for chitosan and larval gut extraction[11].

Chitosan and gut extract preparation: Chitosan was prepared from the third instar larvae by deproteinization, demineralization and deacetylation[12]. The degree of deacetylation (DD) was determined after acid-base titration and determination of the water content[13]. The molecular weight (MW) of chitosan was calculated by the reported viscometric method[14]. Chitosan hydrogel was prepared by dissolving 2% chitosan in 1% (v/v) aqueous acetic acid. Methylparaben sodium salt preservative was added (0.1%, w/w) to the tested samples. Gel was obtained by stirring the resultant solution, followed by sonication to remove excess air bubbles[15]. For gut extraction, egg masses were sterilized, then incubated till hatching. The third instar larvae were dissected, and the extracted crude gut contents were pooled into aliquots and stored at -20°C till used[16].

Experimental mice: The study included one hundred and eighty Swiss Albino mice, four to six weeks old. They were divided into two main groups, wounded non-treated (60 mice) and wounded treated (120 mice) as control group I, and experimental group II respectively. Animals of both groups were equally subdivided into two subgroups: immunocompetent (a) and immunosuppressed (b). Each subgroup of experimental group II was further classified into chitosan treated (1) and gut-treated (2), 30 mice each.

Mice wounding: Just before wounding, mice were anaesthetized by intra-peritoneal injection of ketamine/xylazine cocktail. Mice were wounded on their backs midway between shoulders (1 cm diameter). One millimeter full-thickness skin biopsy specimens from the selected area were aseptically cut from 6 mice in each subgroup after being anaesthetized. For observational wound healing data, specimens were biopsied on the 3rd, 7th, 14th, 21st and 28th days post-wounding (PW) or till complete closure of the wound after being clinically observed for wound healing[17].

Immunosuppression: It was induced in subgroups Ib, IIb1 and IIb2 using cyclophosphamide (Endoxan, purchased from Asta Medica AG, Germany), as 2 intra-peritoneal doses (70 mg/kg each), one week apart for 4 weeks. Wounding was done 48 hours after the second dose. Two extra doses were given at the end of the 2nd and 3rd weeks from the initial dose to maintain the immune suppression state till the end of the experiment (4 weeks)[18].

Application of chitosan and gut extract on mice wounds: A thin layer of the tested compounds was applied daily on wounds using a sterile gauze swab.

Since our study was the first to evaluate larval-derived chitosan and gut extracts, topical application was performed to ensure complete coverage of the wounded area. It was observed that a range of 5-8 aliquots were sufficient to fulfil complete wound covering.

Evaluation of wound healing

Naked eye examination: The efficacy of the tested substances on wound healing was assessed visually to detect the signs of healing and inflammation. These included blistering, swelling, redness, crust formation, bleeding, hair growth, and scar formation[7]. Wound diameter (Di) was also measured to determine wound contractures.

Histopathological study: The quality of wound healing and remodeling process was assessed by examination of stained skin sections taken from the wounded areas at different durations using light microscope (Zeiss, Germany) equipped with camera. Hematoxylin & Eosin (H&E) was used to stain sections for examining the epithelial cells in the epidermis and the dermis[19]. The epidermal thickness was measured using a PathPic image analysis software developed at Alexandria Institute of Medical Researches[20]. Masson's trichrome-stained skin sections were also prepared to evaluate the collagen deposition in the wounded areas. The mean collagen fraction was measured using the ImageJ software (NIH) to compare the amount of collagen in the healed wound between the treated and untreated groups[21,22].

Immunohistochemical study: It was conducted to assess the maturation, differentiation, and proliferation of epithelial cells of the neo-epidermis and neo-dermis after wound healing. Primary antibody (cytokeratin cocktail AE1/AE3) was used to detect the deposition of keratin which is a marker denoting the maturation of keratinocytes[23,24].

Bacteriological study: Quantitative culture technique at different time intervals till the time of complete healing was applied to detect the antibacterial effect of the tested material[25]. Swab specimens for wounds were collected using sterile swabs that were rolled over a wound area of (2x2 cm). Swabs were aseptically placed in a tube containing 5 ml of sterile saline. Tubes were vortexed for 20 seconds. Serial 10-fold dilutions were performed up to a concentration of 10^{-7}. Subsequently, 0.01 ml of each dilution was inoculated on blood agar plate (Oxoid, UK), and incubated aerobically at 37°C for 48 hours. After incubation, the number of bacterial colonies (colony forming unit; CFU) were counted. The total bacterial count was calculated as follows: number of bacterial colonies X the dilution factor X 10. Bacterial colonies were identified according to their colonial morphology on blood agar, Gram-stained films, catalase test, coagulase test and growth on mannitol salt agar[25,26].

Statistical analysis: Data were fed to the computer and analyzed using IBM SPSS software package version 20.0. (Armonk, NY: IBM Corp). Quantitative data were described using range (minimum and maximum), mean, standard deviation and median. The used tests were *F*-test (ANOVA) for normally distributed quantitative variables, to compare between more than two groups, and Post Hoc test (Tukey) for pairwise comparisons. Significance of the obtained results was considered at *P* value less than 0.05.

Ethical considerations: The present study was conducted according to the rules of the Ethics Committee of Alexandria Faculty of Medicine, Egypt. All mice were observed for health status and acclimatized before the experiment at average room temperature of 25°C, 55% humidity and normal photoperiod of day and night. Animals had free access to food and water throughout the experiment.

RESULTS

Chitosan characterization: Results revealed high MW (2,000,000) and high degree of deacetylation (85% DD).

Naked eye examination

1. No signs of local inflammation were detected in wounds of all studied groups. A dry scab was evident on the third day PW in all mice. Complete hair growth with normal skin appearance was observed by the 28th day PW in control immunocompetent mice of Ia subgroup. However, control immunosuppressed mice of Ib subgroup did not achieve this result till the end of the experiment. Similar findings were observed in the corresponding immunocompetent and immunosuppressed chitosan-treated groups (IIa1 and IIb1 respectively). Immunocompetent-gut-treated group (IIa2) showed normal skin and complete hair growth as early as the 14th day PW. However, this was slightly delayed till the 28th day PW in the immunosuppressed group (IIb2).

2. The initial wound expansion observed in all subgroups other than chitosan-treated ones started to contract as early as the 1st day PW. Starting from the 7th day PW, mice in all studied subgroups showed the same rate of wound contraction until wound closure. Complete wound closure was achieved on the 14th day PW in all studied groups except immunocompetent-chitosan-treated IIa1 subgroup that achieved closure as early as the 10th day PW (Fig. 1).

3. Mean Di in immunocompetent control group Ia reached 1.20±0.26 cm and 0.87±0.24 cm on the 3rd and 7th days PW, respectively. Versus the control group, a significant reduction in Di was recorded in subgroup immunocompetent-chitosan-treated

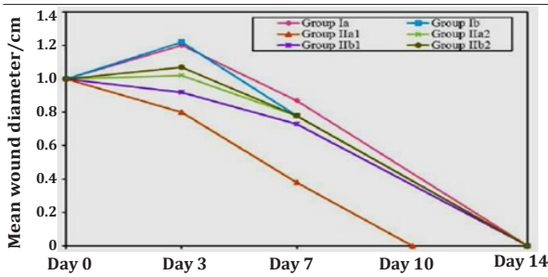

Fig. 1. Progress of wound closure in the studied subgroups.

IIa1 on the 3rd day (0.80±0.14 cm) and the 7th day (0.38±0.15 cm). However, gut extract treatment in immunocompetent IIa2 mice did not achieve a statistical significance in Di reduction. By comparing the treated immunocompetent subgroups, we recorded that the Di was significantly diminished with the use of chitosan treatment in subgroup IIa1 on the 7th day PW (0.38±0.15 cm), compared to 0.78±0.08 cm for gut-treated subgroup IIa2 (Table 1). As regards immunosuppressed subgroups, non-significant reduction in Di was observed in chitosan and gut treated subgroups IIb1 and IIb2 respectively, versus the control group Ib. Similarly, reduction was insignificant between IIb1 and IIb2. Comparison between competent and suppressed subgroups showed that the only Di significant reduction was detected in immunocompetent-chitosan-treated IIa1 subgroup versus the immunosuppressed-gut treated IIb1 subgroup by the 7th day PW (Table 1).

Histopathological results and epidermal remodeling: The H&E-stained skin sections from immunocompetent control group Ia showed thickened epidermis at the wound edges starting from the 3rd day PW overlying cellular granulation tissue (Fig. 2a). An epidermal tongue started creeping across the underlying granulation tissue on the 7th day PW (Fig. 2b). By the 14th day PW, complete re-epithelialization occurred with subsequent wound closure. A line of demarcation was evident between the typical and the neo-dermis (Fig. 2c). Few hair follicles and sebaceous glands appeared on the 21st day PW, until a typical normal skin appearance was encountered by the 28th day PW (Fig. 2d).

In chitosan-treated immunocompetent subgroup IIa1, a creeping tongue composed of disorganized epithelium extending towards the wound margins, was evident earlier on the 3rd day PW. The underlying connective tissue showed hypercellular granulation (Fig. 3a). Subsequently, complete re-epithelialization with hyperkeratotic epidermis was detected on the 7th day PW (Fig. 3b). By the 14th day PW, significant epidermal thickness (Eth) reduction was noticed versus control immunocompetent subgroup Ia, which denoted complete remodeling (Table 2). However, only few hair follicles and sebaceous glands were observed (Fig. 3c). These started to increase in number until normal skin was encountered on the 28th day PW (Fig. 3d).

Stained skin sections from gut extract-treated immunocompetent subgroup IIa2 showed the best results in the histological progress of wound healing. This was evident by early appearance of the epidermal tongue on the 3rd day PW, formed of a monolayer,

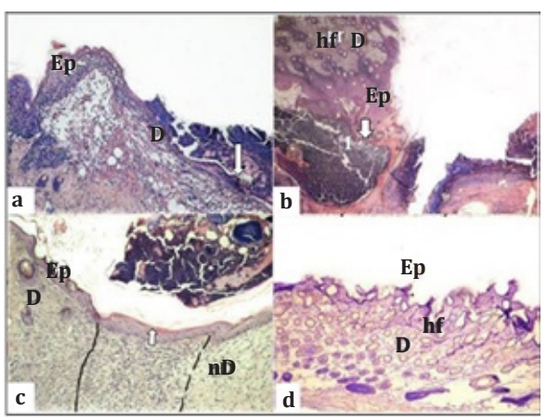

Fig. 2. H&E-stained skin sections of non-treated immunocompetent subgroup (Ia). **a) 3rd day PW:** Thickened epidermis **(Ep)** at the cut edges (arrow) overlying immature hypercellular granulation tissue (×40). **b) 7th day PW:** Migratory epidermal tongue (arrow) penetrating the wound bed. Immature granulation tissue underneath is occupied by infiltrating inflammatory cells **(I)** (×40). **c) 14th day PW:** Complete re-epithelialization with slightly thickened layer (arrow). The neo-dermis **(nD)** is lightly stained with evident demarcation lines separating it from vital tissue (dashed line) and from typical dermis **(D)** (continuous line) (×100). **d) 28th day PW:** Nearly normal control image with excess hair follicles **(hf)** and sebaceous glands (×100).

Table 1. Mean wound diameter (cm) in the studied subgroups.

Days		Immunocompetent subgroups			Immunosuppressed subgroups			Statistical analysis	
		Ia	IIa1	IIa2	Ib	IIb1	IIb2	*F*	*P*
3rd	Mean±SD	1.20±0.26	0.8±0.14	1.02±0.18	1.22±0.26	0.92±0.08	1.07±0.15	4.366*	0.004*
	Significance	***P*1=0.011*; *P*2=**0.558; ***P*3=**0.096; ***P*4=**0.744; ***P*5=**1.000; ***P*6=**0.891; ***P*7=**0.997; ***P*8=**0.377; ***P*9=**0.744							
7th	Mean±SD	0.87±0.24	0.38±0.15	0.78±0.08	0.78±0.12	0.73±0.12	0.78±0.08	8.822*	<0.001*
	Significance	***P*1<0.001*; *P*2=**0.907; ***P*3=**0.989; ***P*4=**1.000; ***P*5=**0.907; ***P*6=0.002*; *P*7=**1.000; ***P*8<0.001*; *P*9=**0.989							

SD: Standard of deviation; ***F, P***: Values for ANOVA test; **Significance:** Between subgroups using Post Hoc Test (Tukey), ***:** Significant (*P*≤0.05), ***P*1:** Between Ia and IIa1, ***P*2:** Between Ia and IIa2, ***P*3:** Between Ib and IIb1; ***P*4:** Between Ib and IIb2; ***P*5:** Between Ia and Ib; ***P*6:** Between IIa1 and IIb1; ***P*7:** Between IIa2 and IIb2; ***P*8:** Between IIa1 and IIa2; ***P*9:** Between IIb1 and IIb2.

progressively followed by a bilayer (formed part) and a disorganized multilayered epithelium towards the wound margin. An evident line of demarcation appeared between the old and neo-dermis indicating good remodeling of the extracellular matrix, and another line separated it from active granulation tissue underlying the wound that appeared earlier than the other two competent groups (Fig. 4a, b). Evident Eth reduction (190.19±52.72) (Table 2), denoting partial remodeling was detected by the 7th day PW (Fig. 4c). Subsequently, complete remodeling was achieved on the 14th day PW with significant reduction in Eth as compared to the Ia immunocompetent control group (Table 2). At the same time, excessive hair follicles and sebaceous glands appeared in the dermis (Fig. 4d). A typical normal skin section was evident by the 21st day PW.

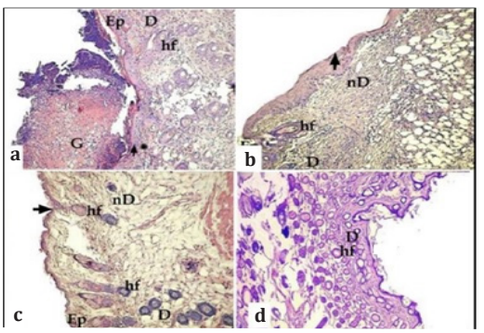

Fig. 3. H&E-stained skin sections of chitosan treated immunocompetent subgroup (IIa1) **a) 3rd day PW:** Epidermal tongue of disorganized creeping epithelium penetrating the wound bed (arrow). The underlying connective tissue shows hyper-cellularity **(*)**. Granulation tissue **(G)** protruded through the wound edges (×40). **b) 7th day PW:** Complete re-epithelialization with thickened hyperkeratotic neo-epithelium (arrow). No associated hair follicles seen in the wound bed (×100). **c) 14th day PW:** Normal looking neo-epidermis (arrow) overlying narrow neo-dermis with limited number of hair follicles in the dermis (×40). **d) 28th day PW:** Nearly normal control image in both epidermis **(Ep)** and dermis with marked number of hair follicles and sebaceous glands (×100).

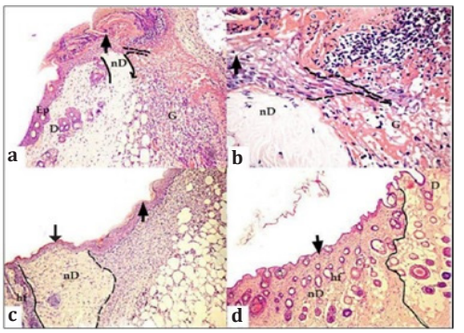

Fig. 4. H&E-stained skin sections of gut-extract treated immunocompetent subgroup (IIa2): **(a, and b) 3rd day PW:** Definite migratory epidermal tongue extending from the neo-epidermis penetrating the wound bed towards the wound edges (dashed line). Definite lines of demarcation between the neo-dermis and both ordinary dermis (continuous line) and granulation tissue (curved arrow) (a×40) (b×100). **c) 7th day PW:** Completely remodeled zone (thin arrow) and a thicker hyperkeratotic zone (thick arrow) in the neo-epidermis. Definite lines of demarcation separating the neo-dermis from both the typical dermis and active granulation tissue (×40). **d) 14th day PW:** Normal looking epidermis (arrow) overlying mature dermal bed rich in hair follicles and sebaceous glands **(hf)**. The neo-dermis is evidently demarcated (continuous line) (×40).

Table 2. Mean epidermal thickness (pixels) in the studied subgroups.

	Days	Immunocompetent subgroups			Immunosuppressed subgroups			Statistical analysis	
		Ia	IIa1	IIa2	Ib	IIb1	IIb2	*F*	*P*
7th	Mean ±SD	306.02 126.12	246.52 68.77	190.19 52.72	352.62 139.90	306.40 107.93	185.02 28.06	3.041*	0.025*
	Significance	***P*1**=0.888; ***P*2**=0.321; ***P*3**=0.959; ***P*4**=0.052; ***P*5**=0.957 ***P*6**=0.886; ***P*7**=1.000**; *P*8**=0.909**; *P*9**=0.273							
14th	Mean ±SD	191.55 39.61	99.37 40.09	57.80 14.26	263.64 89.55	229.07 63.31	130.07 30.14	13.903*	<0.001*
	Significance	***P*1=0.048*; *P*2=0.001*; *P*3=0.857; *P*4=0.001*; *P*5=0.190 *P*6=0.002*; *P*7=0.188; *P*8=0.738 ; *P*9=0.028***							

SD: Standard of deviation; ***F, P*:** Values for ANOVA test; **Significance:** Between subgroups using Post Hoc Test (Tukey), ***:** Significant (*P*≤0.05), ***P*1:** Between Ia and IIa1, ***P*2:** Between Ia and IIa2, ***P*3:** Between Ib and IIb1; ***P*4:** Between Ib and IIb2; ***P*5:** Between Ia and Ib; ***P*6:** Between IIa1 and IIb1; ***P*7:** Between IIa2 and IIb2; ***P*8:** Between IIa1 and IIa2; ***P*9:** Between IIb1 and IIb2.

In immunosuppressed control group Ib, thickened vacuolated epidermis with pyknotic nuclei appeared at the edges of the wound on the 3rd day PW, overlying slightly cellular granulation tissue (Fig. 5a). The Eth was markedly increased on the 7th day PW (352.62±139.90) (Table 2, Fig. 5b). On the 14th day PW, the wound was closed with slightly thickened and vacuolated epidermis (Fig. 5c). Normal epidermis was noticed on the 21st day PW, but with no hair follicles and sebaceous glands till the 28th day PW (Fig. 5d).

In chitosan-treated immunosuppressed subgroup IIb1, thickened vacuolated epidermis similarly appeared on the 3rd day PW (Fig. 6a), as in control subgroup Ib. Complete re-epithelialization was achieved on the 7th day PW (Fig. 6b). Closure of the wound with diminished Eth and vacuolization were noticed by the 14th day PW. Excessive angiogenesis was observed in the dermis but with no hair follicles and sebaceous glands (Fig. 6c). The Eth at that point was decreased, however, it was significantly thicker

than that encountered in immunocompetent-chitosan-treated subgroup IIa1 (Table 2). Angiogenesis started to decrease on the 21st day PW. Skin appendages started to appear in few numbers on the 28th day PW (Fig. 6d).

As in the immunocompetent-gut extract -treated subgroup IIa2, the immunosuppressed-gut extract-treated subgroup IIb2 showed a creeping epidermal tongue as early as the 3rd day PW (Fig. 7a, b), and complete re-epithelialization on the 7th day PW (Fig. 7c). Remodeling and significant decrease in Eth, compared to control immunosuppressed subgroup Ib, were evident on the 14th day PW (Table 2), together with the appearance of hair follicles in the dermis (Fig. 7d). Normal skin section was evident by the 21st day PW.

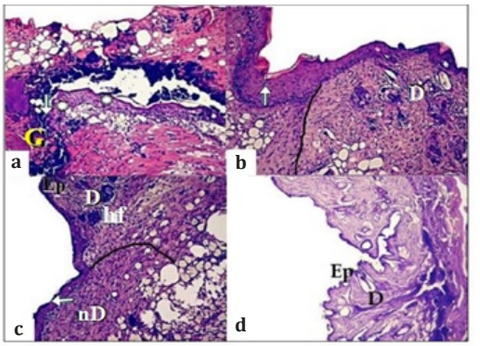

Fig. 5. H&E-stained skin sections of non-treated immunosuppressed subgroup (Ib): **a) 3rd day PW:** Vacuolated epidermal cells (white *) and pyknotic cells extending behind the thickened edges of the wound (arrow). Highly cellular granulation tissue **(G)** is protruding through the wound and the dermis is oedematous (×40). **b) 7th day PW:** Highly thickened epidermis near the opened wound with evident hyperkeratosis and vacuolated cells (arrow). An evident line of demarcation between the typical dermis **(D)** and active zone (continuous line) is formed (×100). **c) 14th day PW:** Healed wound with thickened neo-epidermis (arrow), and vacuolated cells. The underlying neo-dermis **(nD)** is highly cellular and devoid of hair follicles **(hf)**. The line of demarcation is still evident (continuous line) (×40). **d) 28th day PW:** Absence of hair follicles and sebaceous glands (×100). **Ep:** Normal epithelium, **D:** Dermis of normal skin.

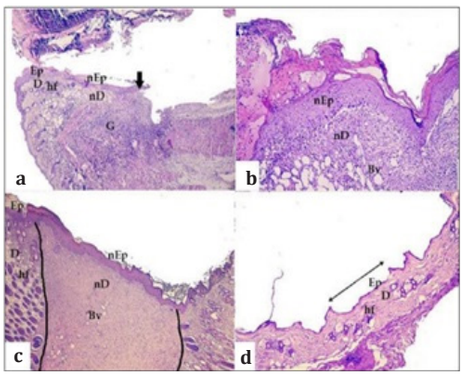

Fig. 6. H&E-stained skin sections of chitosan treated immunosuppressed subgroup (IIb1) **a) 3rd day PW:** Epidermal tongue extending over the wound bed (arrow) with thickened vacuolated neo-epidermis **(nEp)**, a very narrow neo-dermis **(nD)** covering, and excessive cellular granulation tissue **(G)** protruding through wound's edges (×40). **b) 7th day PW:** Complete closure by thickened vacuolated disorganized epidermal cells **(nEp)** overlying neo-dermis **(nD)** and formed mainly of cellular highly vascularized **(BV)** granulation tissue (×100). **c) 14th day PW:** Slightly thickened neo-epidermis **(nEp)** overlying the high cellular neo-dermis with no associated hair follicles. Lines of demarcation are present between typical dermis and vital zone (continuous line) and between the neo-dermis **(nD)** and granulation tissue (continuous line) (×40). **d) 28th day PW:** Normal looking epidermis (double arrow) with moderate number of hair follicles and sebaceous glands. **Ep:** Normal epithelium; **D:** Dermis; **hf:** Hair follicle.

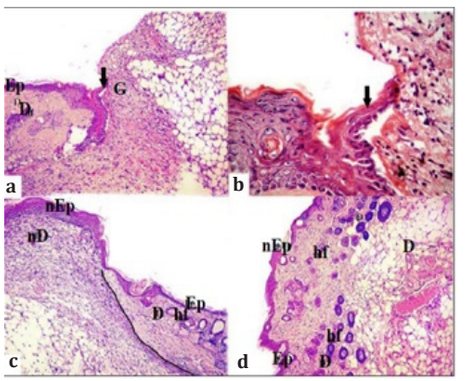

Fig. 7. H&E-stained skin sections of gut treated immunosuppressed subgroup (IIb2): **a and b) 3rd day PW:** Disorganized cellular epidermal tongue creeping over the wound bed (arrow). The epidermis **(Ep)** at the wound edge is slightly thickened. The wound bed is occupied by highly cellular granulation tissue **(G)** (a×40) (b×100). **D:** dermis. **c) 7th day PW:** Complete closure of the wound by thickened hyperkeratotic neo-epidermis **(nEp)** overlying the cellular neo-dermis **(nD)**. Line of demarcation is evident between the neo-dermis and the typical dermis **(D)** (continuous line) (×40). **d) 14th day PW:** Irregularly thickened neo-epidermis **(nEp)** with few hair follicles **(hf)** (×40). **D:** Dermis.

Collagen deposition and Masson's trichrome histopathological results: The best results in collagen deposition were detected in gut treated subgroups. Mean collagen fraction was significantly increased in immunocompetent subgroup IIa2 (226.99±8.55) compared to control subgroup Ia that showed a mean collagen fraction of (184.53±12.96). On the other hand, in immunosuppressed gut treated mice, there was a significant increase in the mean collagen fraction in subgroup IIb2 and its corresponding control (Ib) [the mean collagen fraction was (196.99±10.28) and (118.97±1.57), respectively]. The only significant increase in the mean collagen fraction in chitosan treated mice was detected in immunosuppressed subgroup IIb1 (188.42±16.29) when compared with its immunosuppressed control subgroup Ib (118.97±1.57). On comparing treated immunocompetent and suppressed groups, we recorded a significant difference in mean collagen fraction and in the control non treated groups there was significant increase in collagen fraction in subgroup Ia versus Ib (Table 3).

Table 3. Mean collagen fraction in the studied subgroups.

Days		Immunocompetent subgroups			Immunosuppressed subgroups			Statistical analysis	
		Ia	IIa1	IIa2	Ib	IIb1	IIb2	*F*	*P*
14th	Mean	184.53	212.28	226.99	118.97	188.42	196.99	32.147*	<0.001*
	±SD	12.96	12.88	8.55	1.57	16.29	10.28		
	Significance	***P***1=0.093***; P*2=0.007*; *P*3=<0.001*; *P*4=<0.001*; *P*5=<0.001*** ***P***6=0.181***; P***7=0.063***; P***8=0.625***; P***9=0.934							

SD: Standard of deviation; ***F, P*:** Values for ANOVA test; **Significance:** Between subgroups using Post Hoc Test (Tukey), ***:** Significant ($P \leq 0.05$), ***P*1:** Between Ia and IIa1, ***P*2:** Between Ia and IIa2, ***P*3:** Between Ib and IIb1; ***P*4:** Between Ib and IIb2; ***P*5:** Between Ia and Ib; ***P*6:** Between IIa1 and IIb1; ***P*7:** Between IIa2 and IIb2; ***P*8:** Between IIa1 and IIa2; ***P*9:** Between IIb1 and IIb2.

Similarly, the best histopathological result in terms of collagen fibers deposition was in favor of gut extract treatment (Fig. 8). Subgroup IIa2 showed excessive lightly stained neo-collagen under the remodeled neo-epidermal zone seven days PW, while highly cellular less fibrous granulation tissue with few lightly stained collagen fibers were encountered underneath the healed thickened neo-epidermal zone (Fig. 8e). Stained sections 14 days PW showed increased amount of lightly stained neo-collagen alternating with darker mature deposition in the dermis underneath the apparently normal epidermis (Fig. 8f). Masson's trichrome-stained skin sections obtained from subgroup Ia showed few lightly stained collagen fibers by the 7th day PW, that became denser and horizontally aligned on the 14th day PW (Fig. 8a, b). These observations were similar in chitosan-treated subgroup IIa1 (Fig. 8c, d). Immunosuppressed untreated subgroup Ib, showed immature, lightly stained collagen fibers on the 7th day PW, that remained disorganized till the 14th day (Fig. 8g-i). Chitosan and gut extract treatment of immunosuppressed mice produced significant increase of collagen fibers deposition in the wound bed when compared to sections of untreated mice (Fig. 8j-l). After the 14th day PW, no histological differences were encountered between the studied groups in terms of collagen deposition.

Immunohistochemical results: Keratin-immunostaining reaction of normal skin reflected strong reaction depicted by dark brown staining of the epidermal layers especially in the stratum corneum, and in the hair follicles and lining of blood vessels in the dermis (Fig. 9a). In immunocompetent non-treated subgroup (Ia), keratin immunostaining was recorded only on the 14th day PW samples where the re-epithelialized skin showed very weak reaction (scant brown

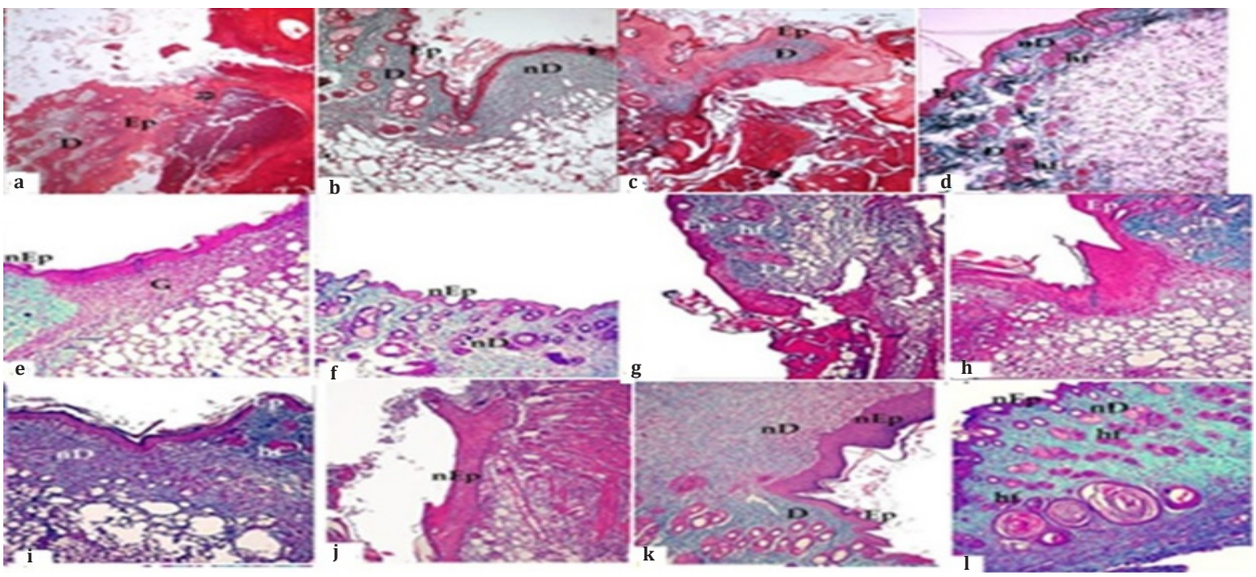

Fig. 8. Fig. 8. Masson's trichrome-stained skin sections of studied animal groups. **a. Group Ia: 7 d PW:** No collagen deposition at the wound area (×100). **b. Group Ia: 14 d PW:** Lightly stained neo-collagen in the neo-dermis underneath the newly thickened re-epithelialized layer (double arrows) (×100). **c. Group IIa1: 3 d PW:** No collagen deposition at the wound site (×100). **d. Group IIa1: 14 d PW:** Mature darkly stained collagen (×100). **e. Group IIa2: 7 d PW:** Excessive lightly stained neo-collagen underneath the remodeled neo-epidermis **(*)**. Few lightly stained neo-collagen fibers (narrow arrow) seen within the highly cellular granulation tissue (×100). **f. Group IIa2: 14 d PW:** Mature darkly stained collagen (×100). **g, h. Group Ib: 3 and 7 d PW:** No collagen deposition at the wound site (×100). **i. Group Ib: 14 d PW:** Collagen intensification (×100). **j. Group IIb1: 3 d PW:** No collagen deposition at the wound site (×100). **k. Group IIb1: 14 d PW:** Intense collagen staining (×100). **l. Group IIb2: 14 d PW:** Intense collagen staining (×100). **Ep:** Normal epithelium; **nEp:** Neo-epithelium; **D:** Dermis; **nD:** Neo-dermis; **hf:** Hair follicle; **G:** Granulation tissue.

color) as compared to the rest of unwounded skin (Fig.9 b). Immunohistochemical results in the present study showed that immunocompetent subgroups IIa1 (chitin-treated) and IIa2 (gut extract-treated) gave the best keratinocyte maturation, demonstrated by the deep brown colour of keratin detected as early as seven days PW in IIa2 (Fig. 9 c-f). Control subgroup Ib showed weak reaction detected as scanty brown colour denoting improper keratin deposition (Fig.9 g, h). Chitosan treated immunosuppressed mice (IIa1) showed lighter reaction (brown colour) till the end of the experiment (Fig.9 i, j). As in the immunocompetent subgroups, gut extract-treated immunosuppressed mice showed dense immune reaction on the 7th and 14th days PW (Fig. 9 k, l).

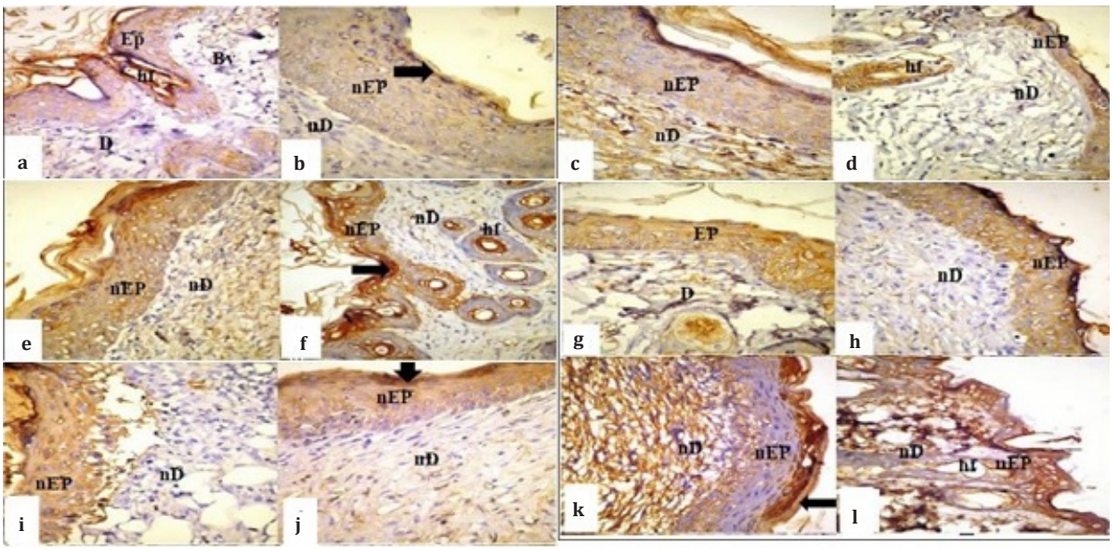

Fig. 9. Immuno-keratin stain of skin sections of control (I) and experimental (II) subgroups. **a)** Normal unwounded skin showing strongly positive reaction (×400). **b) Group Ia: 14th day PW:** Very weak positive reaction in the neo-epidermis (arrow) and the neo-dermis as compared to the rest of unwounded skin (×400). **c) Group IIa1: 7th day PW:** Mild positive reaction (×400). **d) Group IIa1: 14th day PW:** Positive reaction in all epidermal layers as well as the developed hair follicles (×400). **e) Group IIa2: 7th day PW:** Intense positive reaction of the thickened neo-epidermis (×400). **f) Group IIa2: 14th day PW:** More intense positive reaction of the neo-epidermis and the newly formed hair follicles (×400). **g) Group Ib: 3rd day PW:** Asymmetrical positive reaction of the vacuolated epidermal cells at the edge of the wound (×400). **h) Group Ib: 14th day PW:** Positive reaction in the re-epithelialized tissue (×400). **i) Group IIb1: 7th day PW:** Mild positive reaction in the thickened neo-epidermis (×400). **j) Group IIb1: 14th day PW:** More intense reaction in stratum corneum and weak reaction in the neo-dermis (×400). **k) Group IIb2: 7th day PW:** Moderately positive reaction in the neo-epidermis (arrow) (×400). **l) Group IIb2: 14th day PW:** Slightly stronger reaction in the neo-epidermis as well as in the newly formed hair follicles (×400). **Ep:** Normal epithelium; **nEp:** Neo-epithelium; **D:** Dermis; **nD:** Neo-dermis; **hf:** Hair follicle; **G:** Granulation tissue.

Microbiological results: Microbiological study revealed the presence of *Staphylococcus aureus* colonies in opened wounds at different intervals. This was proved by colonial morphology on blood agar plates, grape like clusters of Gram-positive cocci in Gram-stained films, yellow growth on mannitol salt agar, and positive catalase and coagulase reactions. There was significant increase in colonial numbers in control immunosuppressed subgroup Ib (18.36×10^4 ±24.37) compared to control immunocompetent subgroup Ia (1.0×10^4±1.67) on the 7th day PW. While in immunosuppressed chitosan and gut treated mice (IIb1 and IIb2), there was significant reduction in colonial numbers on the 3rd and 7th day PW as compared to control immunosuppressed subgroup Ib. This reduction was not significant between the immunocompetent subgroups (Fig. 10).

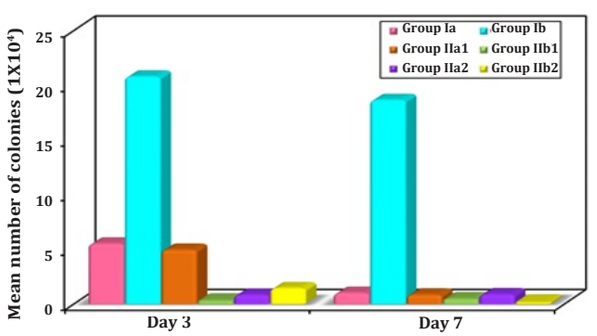

Fig. 10. The mean number of staphylococcal colonies in the studied subgroups, revealing relevant increase in control immunosuppressed non-treated group Ib on the 3rd and 7th days PW.

DISCUSSION

Wound healing in immunosuppressed patients has been recently considered a major global issue that increases the risk of complication of surgical wound healing. The increased prevalence of immunosuppressive states due to the use of chemotherapy or radiotherapy in the field of oncology and the increased demand for organ transplantation, prompted the assessment of wound healing in immunosuppressed condition[27,28]. Anderson and Hamm[29] proved that immunosuppression causes delayed inflammatory phase healing, decreased fibrin deposition and collagen synthesis, and delayed wound contraction[29]. Cyclophosphamide was chosen for the induction of immunosuppression in experimental mice for its known activity in compromising both the cellular and humoral immunity. Cyclophosphamide can inhibit T-lymphocyte proliferation and down regulate clonal expansion and differentiation of B-cells into plasma cells and wound healing process[30,31]. It is worth mentioning that corticosteroids were not used in the present study as a high dose is required to induce immunosuppression in mice according to Mc-Cabe *et al*.[32]. Furthermore, Maubec *et al*.[33] proved that glucocorticoids can cause skin atrophy through their inappropriate occupancy of mineralocorticoid receptors present in the epidermis[33].

Observation of wound contraction in the present studied groups showed that chitosan yielded the best results proved by absence of the initial wound expansion that was observed in all other groups, and with the earliest wound closure on the 10th day PW. This may be attributed to the potential stimulatory effect of chitosan on myofibroblasts. In immunosuppressed chitosan-treated mice (IIb1), complete closure of the wound observed on the 7th day PW was apparently delayed till the 14th day in immunosuppressed non-treated subgroup (Ib). This was expected due to the leucopenia induced by cyclophosphamide and was confirmed by the resulting statistical insignificant reduction in wound size in IIb1 subgroup on the 7th day when compared to their corresponding non-treated subgroup (Ib). Demidova-Rice *et al*.[34] explained that the potential chemoattractant effect of chitosan on inflammatory cells leads to production of several growth factors that fasten wound healing. The present results showed no difference in the duration of wound healing among the studied groups. This may be due to the small wound size (1cm×1cm) that can heal rapidly within almost 14 days. Moreover, two studies[22,35] suggested that wound contraction should not be the sole factor in assessing wound healing in rodents as the healing potential is very high, with immediate contraction of the wound and a high proliferation rate, thus, even critical size wounds close very quickly[22,35]. On the other hand, it was observed that rapid wound closure does not necessarily mean a normal morpho-functional regeneration of skin. Contrarily, disoriented connective tissue could be formed with a deformed fibrous appearance that may cause mechanical redundancy and scar formation[36]. Hence, the current assessment was extended to histopathological examination of skin sections taken at different durations from all subgroups.

Although the creeping neo-epidermis appeared as early as the 3rd day PW in competent treated subgroups IIa1 and IIa2 versus the 7th day in untreated Ia subgroup, gut extract treatment yielded multilayers, with a more organized creeping epidermal tongue when compared to that yielded by chitosan treatment. Hastened remodeling was evidenced by the obvious demarcation between the typical dermis, neo-dermis and the highly cellular granulation tissue on the 7th day PW. Hair follicles and sebaceous glands were abundant starting from the 14th day afterwards, till a typically normal skin section was encountered on the 21st day, that is to say, earlier than chitosan-treated wounds. This structural repair achieved by gut extract was formerly detected by wound inspection for assessment of hair growth (H parameter), where normal hair-covered skin was grossly observed on the 14th day PW in immunocompetent gut treated subgroup IIa2. It is worth mentioning that Lemo *et al*.[35] declared that hair migration is possible only in mature tissues and cannot start except after re-epithelialization is complete. Even in the case of immunosuppression, gut extract treatment was significantly superior over chitosan treatment as it showed complete remodeling with the appearance of skin appendages in the dermis on the 14th day PW, while chitosan treated sections did not achieve normality till the end of the experiment. It was reported that reduction in polymorphonuclear cells occurs at the injury site[28]. This can explain the presence of pyknotic cells and vacuolated eidermis in immunosuppressed control and chitosan-treated groups, Ib and IIb1 respectively. Besides, in the same subgroups there was delay in appearance of hair follicles and sebaceous glands till the end of the 4th week PW. This in turn could directly affect the subunit CD18 molecule that constitutes β2 integrin of the lymphocyte cellular surface which is essential for normal inflammatory response[37].

As regards collagen deposition and keratinocyte activation, chitosan treatment resulted in significantly higher collagen fraction only in immunosuppressed mice as detected in Masson's trichrome-stained sections. This could be explained by the stimulatory effect of chitosan on fibroblasts which are the main source of collagen. Jawad *et al*.[38] suggested that chitosan hydrogel had the capacity to stimulate fibroblastic proliferation that could release interleukin-5 and collagen[38]. Besides, they declared that chitosan could stimulate macrophage migration, and increase effusion that forms thick fibrin.

Moreover, immunohistochemical analysis showed a deep brown colour indicating strong positive reaction to mouse anti-cytokeratin AE1/AE3, by the deposited keratinocytes in the chitosan-treated groups versus their corresponding controls. Here it is worth mentioning that the use of high MW chitosan with high DD was decided to gain benefit from the high solubility of N-acetyl glucosamine molecules. This is in accordance to Jayakumar *et al*.[39] who suggested that the solubility of N-acetyl glucosamine could increase chitosan absorption on topical applications allowing a major effect on the healing process[39]. Moreover, Attia and El-Samad[6] declared that high MW chitosan, with high degree of deacetylation was promising for use as a treatment system for dermal burns[6].

Masson's trichrome staining in subgroups IIa2 and IIb2 (gut extract-treated subgroups) showed intense mature collagen deposition. An increasing amount of alternating light and dark stained neo-collagen fibers underneath the normalized epidermis was observed on the 14th day PW with significant increase in the mean collagen fraction versus non-treated groups. This may be explained by enhancement of the action of several enzymes in the gut of *M. domestica* maggots that appear to have a dramatic role in the process of efficient wound healing and the building of well-formed cutaneous cytoarchitecture. These include several acid proteinases that are restricted to the midguts of *M. domestica* larvae. The pH and gut structure of *M. domestica* larvae can accommodate the presence of these enzymatic secretions and adapt well to them. Cathepsin-D (CD) like activity of gut proteinases was also proved[40]. Egberts *et al*.[41] suggested that CD may be involved in the process of epithelial differentiation, epidermal barrier function and wound healing through activation of transglutaminase-1 (TG-1), which cross-links the proteins of cornified envelope, a structure beneath plasma membrane of keratinocytes, during epidermal differentiation[41].

Zheng *et al*.[42] assumed that the increased amount of CD in the subcutaneous tissue might stimulate transglutaminase (TGase) activity through cellular interaction and signalling and hence the terminal keratinization process[42]. Besides, the significant decrease in epidermal thickness in gut extract-treated mice compared to their corresponding non-treated ones strongly pointed to the activation of keratinocytes by gut extracts and early epidermal remodeling. Consequently, in the present study, strong immunohistochemical staining evident by the 7th and 14th days PW in IIa2 and IIb2 respectively confirmed the early good remodeling detected by H&E and trichrome stains. We suggested that this effect could be attributed to keratinocyte activation represented by keratin formation as previously reported[24].

Several studies threw light on the role of skin keratinocytes in wound healing process through the secretion of numerous proteins that include proteolytic enzymes such as interstitial collagenase[43], matrix metalloproteinases[44], and cathepsin B[45]. These proteolytic enzymes played a role in migration of keratinocytes to peripheral layers of the epidermis and in remodeling in the extracellular matrix. Recruited keratinocytes become activated during epidermal regeneration with production of different cytokines that have a major role in wound healing process. This was further explained by Vashishta *et al*.[46] who described for the first time that keratinocytes also secrete pCD (inactive proform of CD). Their results suggested that the secreted pCD induces secretion of cytokines (IL-4, IL-6, IL-8, IL-10, and IL-13) that help in normal physiological functions such as overcoming stresses and enhancing the regeneration process of wound healing.

The previous findings support our suggestion for the immunomodulatory effect of *M. domestica* larval gut extracts that improved epithelial maturation of wounds in immunosuppressed IIb2 subgroup close to that of their corresponding immunocompetent subgroup. In the present study, immunomodulation, and improvement in wound healing especially in subgroup IIb2 could be explained by cytokines secreted after stimulation of keratinocytes activation.

An important key factor in wound healing is prevention of wound infection, so as not to disturb the normal healing cascade. The present results showed bacterial wound colonization in all control and experimental groups, with no macroscopic signs of true infection. This was because the colonial quantification did not exceed 104 CFU/g in all studied groups. According to Asada *et al*.[47], the average bacterial count in infected wounds showing macroscopic signs of infection should reach 109 CFU/g[47]. Macroscopic and microscopic examination of the colonies proved that they belong to *Staphylococcus aureus*. Notably, it is the most abundant skin-colonizing bacteria responsible for most nosocomial and community-associated skin infections[48]. The current results showed a significant higher staphylococcal colonization in immunosuppressed subgroup Ib versus immunocompetent subgroup Ia on the 3rd and 7th days PW. This emphasized the neutropenic effect of cyclophosphamide on immunosuppressed mice, especially as neutrophils have the most important role in eliminating the invading bacteria and are the first to arrive at the site of infection[49]. Furthermore, treatment of immunosuppressed animals with topical chitosan (IIb1) and gut extracts (IIb2) showed evident significant reduction in the number of bacterial colonies compared to non treated subgroup Ib. As confirmed by Rabea *et al*.[50], the antimicrobial action of chitosan could be assigned to its high MW that allowed for high DD and in turn higher positively charged amines that could disrupt the negatively charged bacterial membrane.

As regards gut larval extracts, the antibacterial effect could be explained by the presence of lysozymes and CD-like proteinase that catalyze the hydrolysis of the 1,4-beta-glycosidic linkage between N-acetylmuramic acid and N-acetylglucosamine of the peptidoglycan present in the cell wall of many bacteria. This was also recounted by Padilha *et al*.[40]. Curiously, it was proved that flies are the only animals, other than vertebrates, that display an acidic region in their midgut, thus could digest bacteria as in vertebrates[51]. While the presence of antibacterial peptides with a MW of approximately 3-20 kDa that can be isolated from various insects, two studies[52,53] were published on antibacterial compounds with a MW of less than one kDa. This antibacterial activity of *M. domestica* (451 Da) was detected in the whole body extracts, haemolymph, and maggot excretions[52]. Huberman *et al*.[53] assumed that the same active compounds found in the body of maggots are also contained in its excretions. The investigators also proved that the antibacterial molecules with a MW of less than one kDa have an immediate response and may thus be considered a first line defense mechanism against the intrusion of bacteria. This leads us to the reasonable justification of the antibacterial effect of *M. domestica* larvae gut secretion especially in immunosuppressed mice.

In conclusion, the marvelous effect of gut extracts could be a new light in the field of wound healing. Mature and intense collagen deposition was observed in mice treated with the presented new extract. Additionally, it had antibacterial effect, evident in reducing the colonial count, thus protecting against wound infection that can be a major threat against healing especially in immunosuppressed mice. On the other hand, chitosan was superior in wound closure acceleration. Its effect was mainly evident in immunocompetent subgroup. Furthermore, the antibacterial effect of chitosan was evident by colonial number reduction in competent and suppressed subgroups. The delay in hair growth in chitosan treated subgroups besides, the poor epidermal remodeling at the time of wound closure could be a defect in tissue repair especially in immunosuppressed subgroup. The benefits of chitosan should be outweighed versus its drawbacks when considering it for wound healing during immunosuppression. This should enhance further investigation interpreting the effect of possible combination therapy including the two extracts. The present results opened a new field using *M. domestica* larval extracts as a relevant and reliable substitute to that of the famous *L. sericata* larvae in the field of maggot therapy.

Author' contribution: Said DE founded the research idea, revised the data and the manuscript. Khalifa HM conducted the histopathological study and interpretation of histopathological results. El-Samad LM supervised the rearing of *M. domestica* and processing of maggots for extraction of chitin and gut extracts, and the preparation of chitosan. Meheissen MA supervised the microbiological study and revision of results. Diab HE carried out the practical part including animal wounding, preparation of chitosan, follow-up of wounded animals, writing the manuscript. Diab RG conducted and supervised the experiment and revised the manuscript. All authors approved the final version before publication.

Conflict of interest: Authors declare that there is no any conflicts of interest.

Funding statement: The work was completely done in our laboratories without external funds.

REFERENCES

1. Sherman RA. Mechanisms of maggot-induced wound healing: What do we know, and where do we go from here? eCAM 2014; 592419.
2. Richardson M. The benefits of larval therapy in wound care. Nurs Stand 2004; 19(7):70-74.
3. Wollina, U, Kartem K, Herold C, Looks A. Biosurgery in wound healing: The renaissance of maggot therapy. J Eur Acad Dermatol Venereol 2000; 14(4):285-289.
4. Ong SY, Wu J, Moochhala SM, Tan MH, Lu J. Development of a chitosan-based wound dressing with improved hemostatic and antimicrobial properties. Biomaterials 2008; 29(32):4323-4332.
5. Zhang AJ, Qin QL, Zhang H, Wang HT, Li X, Miao L, *et al*. Preparation and characterisation of food-grade chitosan from housefly larvae. Czech J Food Sci 2011; 6(29):616–623.
6. Attia AA, El-Samad LM. Application of hydrogel chitosan extract from the house fly (*Musca domestica vicina*) on burn wound healing of mice. IJAR 2015; 3(9):84-94.
7. Liang D, Lu Z, Yang H, Gao J, Chen R. Novel asymmetric wettable AgNps/chitosan wound dressing: *In vitro* and *in vivo* evaluation. ACS Appl Mater Interfaces 2016; 8(6):3958-3968.
8. Andersen AS, Sandvang D, Schnorr KM, Kruse T, Neve S, Joergensen B, *et al*. A novel approach to the antimicrobial activity of maggot debridement therapy. J Antimicrob Chemother 2010; 65(8):1646-1654.
9. Rosen DJ, Patel MK, Freeman K, Weiss PR. A primary protocol for the management of ear keloids: results of excision combined with intraoperative and postoperative steroid injections. Plast Reconstr Surg 2007; 120(5):1395-1400.
10. Čičková H, Newton GL, Lacy RC, Kozánek M. The use of fly larvae for organic waste treatment. Waste Management 2015; 35:68-80.
11. Mumcuoglu KY, Ingber A, Gilead L, Stessman J, Friedmann R, Schulman H, *et al*. Maggot therapy for the treatment of intractable wounds. Int J Dermatol 1991; 38(8):623-627.
12. Sarbon NM, Sandanamsamy S, Kamaruzaman SF, Ahmad F. Chitosan extracted from mud crab (*Scylla olivicea*) shells: Physicochemical and antioxidant properties. J Food Sci Technol 2015; 52(7):4266-4275.
13. Kjartansson GT. Extraction and functional properties of ultrasonicated chitin and chitosan from crustacean

by-products. Ph.D. Thesis, University of Massachusetts Amherst; MA, USA, 2008.
14. Zhang H, Neau SH. *In vitro* degradation of chitosan by a commercial enzyme preparation: Effect of molecular weight and degree of deacetylation. Biomaterials 2001; 22:1653–1658.
15. Alsarra IA. Chitosan topical gel formulation in the management of burn wounds. Int J Biol Macromol 2009; 45(1):16-21.
16. Thyssen PJ, Nassu MP, Nitsche MJT, Leite DS. Sterilization of immature blowflies (Calliphoridae) for use in larval therapy. Int J Med Med Sci 2013; 4(10):405-409.
17. Midwood KS, Williams LV, Schwarzbauer JE. Tissue repair and the dynamics of the extracellular matrix. Int J Biochem Cell Biol 2004; 36(6):1031-1037.
18. McCormick S, Dowler K, Armstrong JA, Hsiung GD. Cyclophosphamide immunosuppression during lymphotropic Herpes virus infection in the guinea pig model. A histopathologic and virologic study. Am J Pathol 1987; 127(3):538-548.
19. Bancroft JD, Gamble M. Theory and practice of histological techniques. 5th ed. London: Churchill Livingstone; 2002.
20. Alper M, Kavak A, Parlak AH, Demirci R, Belenli I, Yesildal N. Measurement of epidermal thickness in a patient with psoriasis by computer-supported image analysis. Braz J Med Biol Res 2004; 37(1):111-117.
21. Kiernan JA. Histological and histochemical method (theory and practice), 4th ed. 2008; United Kingdom: Scion Publishing.
22. Mehanna RA, Nabil I, Attia N, Bary AA, Razek KA, Ahmed TAE, *et al*. The effect of bone marrow-derived mesenchymal stem cells and their conditioned media topically delivered in fibrin glue on chronic wound healing in rats. Biomed Res Int 2015; 846062.
23. Petrosyan K, Tamayo R, Joseph D. Sensitivity of a novel biotin-free detection reagent (power vision+) for immunohistochemistry. J Histotechnol 2002; 25:247-250.
24. Erwin, Etriwati, Gunanti, Handharyani, E, Noviana D. Changes in histopathology and cytokeratin AE1/AE3 expression in skin graft with different time on Indonesian local cats. Vet World 2017; 10(6):662-666.
25. Rondas AA, Schols JM, Halfens RJ, Stobberingh EE. Swab versus biopsy for the diagnosis of chronic infected wounds. Adv Skin Wound Care 2013; 26(5):211-219.
26. Tavares DS, Lima-Ribeiro MH, de Pontes-Filho NT, Carneiro-Leão AM, Correia MT. Development of animal model for studying deep second-degree thermal burns. J Biomed Biotechnol 2012; 460841.
27. Burkatovskaya M, Castano AP, Demidova-Rice TN, Tegos GP, Hamblin MR. Effect of chitosan acetate bandage on wound healing in infected and noninfected wounds in mice. Wound Repair Regen 2008; 16(3):425-431.
28. de Melo CM, Porto CS, Melo-Júnior MR, Mendes CM, Cavalcanti CC, Coelho LC, *et al*. Healing activity induced by Cramoll 1,4 lectin in healthy and immunocompromised mice. Int J Pharm 2011; 408(1-2):113-119.
29. Anderson K, Hamm RL. Factors that impair wound healing. J Amer College Clin Wound Specialists 2014; 4(4):84-91.
30. Diehl R, Ferrara F, Müller C, Dreyer AY, McLeod DD, Fricke S, *et al*. Immunosuppression for *in vivo* research: State of the art protocols and experimental approaches. Cell Mol Immunol 2017; 14(2):146-179.
31. Baum CL, Arpey CJ. Normal cutaneous wound healing: clinical correlation with cellular and molecular events. Dermatol Surg 2005; 31(6):674-686.
32. Sali A, Guerron AD, Gordish-Dressman H, Spurney CF, Iantorno M, Hoffmanet EP, *et al*. Glucocorticoid-treated mice are an inappropriate positive control for long-term preclinical studies in the mdx mouse. PLoS One 2012; 7(4):e34204.
33. Maubec E, Laouénan C, Deschamps L, Nguyen VT, Scheer-Senyarich I, Wackenheim-Jacobs AC, *et al*. Topical mineralocorticoid receptor blockade limits glucocorticoid-induced epidermal atrophy in human skin. J Investig Dermatol 2015; 135(7):1781-1789.
34. Demidova-Rice TN, Salomatina EV, Yaroslavsky AN, Herman IM, Hamblin MR. Low-level light stimulates excisional wound healing in mice. Lasers Surg Med 2007; 39(9):706-715.
35. Lemo N, Marignac G, Reyes-Gomez E, Lilin T, Crosaz O, Ehrenfest DM. Cutaneous re-epithelialization and wound contraction after skin biopsies in rabbits: A mathematical model for healing and remodeling index. Vet Arh 2010; 80(5):637-652.
36. Takeo M, Lee W, Ito M. Wound healing and skin regeneration. Cold Spring Harb Perspect Med 2015; 5(1):a023267.
37. Sindrilaru A, Seeliger S, Ehrchen JM, Peters T, Roth J, Scharffetter-Kochanek K, *et al*. Site of blood vessel damage and relevance of CD18 in a murine model of immune complex-mediated vasculitis. J Investig Dermatol 2007; 127(2):447-454.
38. Jawad AH, Al-Diab JM, Ibraheem MK. Effect of chitosan sheets on wound healing. Basra J Vet Res 2007; 6(1):82-96.
39. Jayakumar R, Prabaharan M, Sudheesh Kumar PT, Nair SV, Tamura H. Biomaterials based on chitin and chitosan in wound dressing applications. Biotechnol Adv 2011; 29(3):322-337.
40. Padilha MH, Pimentel AC, Ribeiro AF, Terra WR. Sequence and function of lysosomal and digestive cathepsin D-like proteinases of *Musca domestica* midgut. Insect Biochem Mol Biol 2009; 39(11):782-791.
41. Egberts F, Heinrich M, Jensen JM, Winoto-Morbach S, Pfeiffer S, Wickel M, *et al*. Cathepsin D is involved in the regulation of transglutaminase 1 and epidermal differentiation. J Cell Sci 2004; 117(11):2295-2307.
42. Zheng Y, Chen H, Lai W, Xu Q, Liu C, Wu L, *et al*. Cathepsin D repairing role in photodamaged skin barrier. Skin Pharmacol Physiol 2015; 28(2):97-102.
43. Rodrigues M, Kosaric N, Bonham CA, Gurtner GC. Wound healing: A cellular perspective. Physiol Rev 2019; 99(1):665-706.
44. Stamenkovic I. Extracellular matrix remodeling: the role of matrix metalloproteinases. J Pathol 2003; 200(4):448-464.
45. Büth H, Wolters B, Hartwig B, Meier-Bornheim R, Veith H, Hansen M, *et al*. HaCaT keratinocytes secrete lysosomal

cysteine proteinases during migration. Eur J Cell Biol 2004; 83(11-12):781-795.
46. Vashishta A, Ohri SS, Vetvickova J, Fusek M, Ulrichova J, Vetvicka V. Procathepsin D secreted by HaCaT keratinocyte cells: A novel regulator of keratinocyte growth. Eur J Cell Biol 2007; 86(6):303-313.
47. Asada M, Nakagami G, Minematsu T, Nagase T, Akase T, Huang L, *et al*. Novel models for bacterial colonization and infection of full-thickness wounds in rats. Wound Repair Regen 2012; 20(4):601-610.
48. Otto M. *Staphylococcus* colonization of the skin and antimicrobial peptides. Expert Rev Dermatol 2010; 5(2):183-195.
49. Faurschou M, Borregaard N. Neutrophil granules and secretory vesicles in inflammation. Microbes Infect 2003; 5(14):1317-1327.
50. Rabea EI, Badawy ME, Stevens CV, Smagghe G, Steurbaut W. Chitosan as antimicrobial agent: Applications and mode of action. Biomacromolecules 2003; 4(6): 1457-1465.
51. Overend G, Luo Y, Henderson L, Douglas AE, Davies SA, Dow JA. Molecular mechanism and functional significance of acid generation in the *Drosophila* midgut. Sci Rep 2016; 6: 27242.
52. Meylaers K, Clynen E, Daloze D, DeLoof A, Schoofs L. Identification of 1-lysophosphatidylethanolamine (C(16:1)) as an antimicrobial compound in the housefly, *Musca domestica*. Insect Biochem Mol Biol 2004; 34(1):43-49.
53. Huberman L, Gollop N, Mumcuoglu KY, Block C, Galun R. Antibacterial properties of whole-body extracts and haemolymph of *Lucilia sericata* maggots. J Wound Care 2007; 16(3):123-127.